

UMN-TH-2211/03
 FTP-INN-03/22
 August 2003

CP asymmetries in penguin-induced B decays in general left-right models

Soo-hyeon Nam

William I. Fine Theoretical Physics Institute, University of Minnesota,
 Minneapolis, MN 55455, USA

Abstract

We study CP asymmetries in penguin-induced $b \rightarrow sss$ decays in general left-right models without imposing manifest or pseudom manifest left-right symmetry. Using the effective Hamiltonian approach, we evaluate CP asymmetries in $B \rightarrow K^{(*)}$ decays as well as mixing induced B meson decays $B \rightarrow J/\psi K_s$ and $B \rightarrow K_s$ decays. Based on recent measurements revealing large CP violation, we show that nonmanifest type model is more favored than manifest or pseudom manifest type.

1 Introduction

One of the major goals of present experiments in B physics is the study of CP violation which may reside in the quark flavor mixing described by the Cabibbo-Kobayashi-Maskawa (CKM) matrix in the Standard SU(2)_L × U(1) Model (SM). Since there is one complex phase in CKM matrix, the sizes and patterns of CP violation in various decay modes in the SM are in principle expressed through this single parameter [1]. But the present experimental results with large CP violation effects in the B meson system are not simply explained with this single parameter under the minimal SM framework [2]. For instance, the CP asymmetries in mixing induced B meson decays is characterized by a CP angle which is a phase of the CKM matrix element V_{td} , and the observed world average value of $\sin 2\beta$ in $B \rightarrow J/\psi K_S$ ($b \rightarrow c\bar{c}s$) decays is given by

$$\sin 2\beta_{J/\psi K_S} = 0.734 \pm 0.054. \quad (1)$$

Besides, this CP angle is recently measured by BABAR and Belle in $B \rightarrow K_S$ ($b \rightarrow s\bar{s}s$) decays [3], and their average value is

$$\sin 2\beta_{K_S} = 0.39 \pm 0.41. \quad (2)$$

In the SM, however, the CP asymmetry in $B \rightarrow K_S$ decays is expected to be very close to that in $B \rightarrow J/\psi K_S$ decays [4]. Admitting that the statistical error of those experimental data is still large to confirm the data and justify any theory, a 2:7 deviation between $\sin 2\beta_{J/\psi K_S}$ and $\sin 2\beta_{K_S}$ may give a clue of new physics (NP) effects in B decays. If so, other inclusive $b \rightarrow s\bar{s}s$ dominated B decays such as $B \rightarrow K^{(*)}$ decays might receive the same contribution from the NP.

In a recent paper [5], we have investigated the mixing induced CP asymmetry in $B \rightarrow J/\psi K_S$ decays in the general left-right model (LRM) with group SU(2)_L × SU(2)_R × U(1) since it is one of the simplest extensions of the SM gauge group as a complement of the purely left-handed nature of the SM [6]. Due to the extended group SU(2)_R in the LRM there are new neutral and charged gauge bosons, Z_R and W_R as well as a right-handed gauge coupling, g_R . After spontaneous symmetry breaking, the gauge eigenstates W_R mix with W_L to form the mass eigenstates W and W^0 with masses M_W and M_{W^0} , respectively. The W_L – W_R mixing angle and the ratio of M_W^2 to $M_{W^0}^2$ are restricted by a number of low-energy phenomenological constraints along with the right-handed mass mixing matrix elements. From the limits on deviations of muon decay parameters from the V-A prediction,

the lower bound on M_{W^0} can be obtained as follows [7]:

$$g < 0.033 \quad \text{or} \quad M_{W^0} > (g_R = g_L) \quad 440 \text{ GeV}; \quad (3)$$

where $g_L^2 M_W^2 = g_R^2 M_{W^0}^2$. Previously, stronger limits of the mass M_{W^0} as well as the mixing angle were presented by many authors experimentally [8] and theoretically [9] assuming manifest ($V^R = V^L$) or pseudomaniest ($V^R = V^L K$) left-right symmetry ($g_L = g_R$), where V^L and V^R are the left- and right-handed quark mixing matrices, respectively, and K is a diagonal phase matrix [10]. But, in general, the form of V^R is not necessarily restricted to manifest or pseudomaniest symmetric types, so the W_R mass limit can be lowered to approximately 300 GeV by taking the following forms of V^R [11]:

$$V_I^R = \begin{bmatrix} 0 & 1 \\ e^{i1} & 0 \\ 0 & s_R e^{i1} \\ 0 & s_R e^{i3} \end{bmatrix} \begin{bmatrix} B \\ A \end{bmatrix}; \quad V_{II}^R = \begin{bmatrix} 0 & 1 \\ e^{i1} & 0 \\ 0 & s_R e^{i1} \\ 0 & s_R e^{i3} \end{bmatrix} \begin{bmatrix} B \\ A \end{bmatrix}; \quad (4)$$

where $c_R = (s_R) \cos_R (\sin_R) (0_R 90)$. Here the matrix elements indicated as 0 may be $\sim 10^2$ and unitarity requires $c_1 + c_4 = c_2 + c_3$. From the b! c semileptonic decays of the B mesons, we can get an approximate bound $|g \sin_R| \sim 0.013$ by assuming $|j_{cb}^L| \sim 0.04$ [12], where $g = (g = g_L)^{-1}$. This new parameter g is in general smaller than the charged gauge boson mass ratio g in the general LR M [5, 9]. In a similar way to the charged gauge bosons, the neutral gauge bosons mix each other [13]. But we do not present them here because Z_R contribution to penguin-induced B decays is negligible. Also, due to gauge invariance, tree-level flavor-changing neutral Higgs bosons with masses M_H enter into our theory [14]. However, we also neglect their contributions by assuming $M_H \gg M_W$.

The CP asymmetry in the penguin-induced $B \rightarrow K_S$ decays was also studied earlier in the pseudomanifest left-right symmetry model in Ref. [15]. In this case, the right-handed current contribution to BB mixing is suppressed by $\frac{1}{2}$ so that the NP effect only arises in the magnetic penguin since the suppression by $\frac{1}{2}$ is offset by a large factor $m_t = m_b$ arising in the virtual top quark loop [16]. However, in the nonmanifest LRM, $\frac{1}{2}$ terms in BB mixing and absorptive part of the decay amplitudes become important due to the possible enhancement of V^R elements so that the right-handed current contribution to the corresponding CP asymmetry is more enhanced. In this paper, as a continuation of our previous work, we will explicitly evaluate the possible right-handed current contribution to

¹In Ref. [5], g is defined as $(g_L = g_R)$ unlike this paper so that the mistakenly written bound $g \sin \theta_R \leq 0.013$ should read $(g_R = g_L) \sin \theta_R \leq 0.013$.

CP asymmetry in $B \rightarrow K^{(*)}$ decays as well as in $B \rightarrow K_S$ decays in the general LRM related to recent measurements, and show that CP asymmetries in those decays can be large enough to probe the existence of the right-handed current using the effective Hamiltonian approach. After reviewing the structure of the effective Hamiltonian in the general LRM in Sec. 2, we will discuss CP asymmetries in the several b! sss dominated B decays in Sec. 3 in detail.

2 Effective Hamiltonian

The low-energy effects of the full theory can be described by the effective Hamiltonian approach in order to include QCD effects systematically. The low-energy effective Hamiltonian calculated within the framework of the operator product expansion (OPE) has a finite number of operators in a given order, which is dependent upon the structure of the model. In the LRM, the low energy effective Hamiltonian at the energy scale for $B \rightarrow 1$ and $S \rightarrow 1$ transition has the following form :

$$H_{\text{eff}} = \frac{G_F}{2} \sum_{\substack{i=1,2 \\ q=u,c}}^{\text{hX}} C_i^q O_i^q + \frac{G_F}{2} \sum_{i=3}^{\text{X}^2} (C_i O_i + C_7 O_7 + C_8^G O_8^G) + (C_i O_i + C_i^0 O_i^0); \quad (5)$$

where $\frac{A^B}{q} = V_{qs}^A V_{qb}^B$, $O_{1,2}$ are the standard current-current operators, $O_3 \dots O_{10}$ are the standard penguin operators, and O_7 and O_8^G are the standard photonic and gluonic magnetic operators, respectively, which can be found in Ref. [17]. Since we have additional $SU(2)_R$ group in the LRM, the operator basis is doubled by O_i^0 which are the chiral conjugates of O_i . Also new operators $O_{11,12}$ and $O_{11,12}^0$ arise with mixed chiral structure of $O_{1,2}$ and $O_{1,2}^0$ [16].

In order to calculate the Wilson coefficients $C_i(\mu)$, we first calculate them at $\mu = M_W$ scale. After performing a straightforward matching computation, we find the Wilson coefficients at M_W scale neglecting the u-quark mass:

$$\begin{aligned} C_2^q(M_W) &= 1; \quad C_2^{q0}(M_W) = -g_q^{RR} = -\frac{L_L}{q}; \\ C_7(M_W) &= F(x_t^2) + A^{tb} F(x_t^2); \\ C_7^0(M_W) &= A^{ts} F(x_t^2); \\ C_8^G(M_W) &= G(x_t^2) + A^{tb} G(x_t^2); \\ C_8^{G0}(M_W) &= A^{ts} G(x_t^2); \end{aligned} \quad (6)$$

where

$$x_q = \frac{m_q}{M_W} \quad (q = u; c; t); \quad A^{\text{td}} = \frac{m_t}{m_b} \frac{V_{\text{td}}^R}{V_{\text{td}}^L} e^i \quad (D = b; s); \quad (7)$$

and δ_i is a CP phase residing in the vacuum expectation values, which can be absorbed in θ_i in Eq. (4) by redefining $\theta_i + \delta_i \rightarrow \theta_i$. All other coefficients vanish. In Eq. (6), the explicit forms of the functions $F(x_t)$, $F^{\text{e}}(x_t)$, $G(x_t)$, and $G^{\text{e}}(x_t)$ are given in Ref. [16], and the terms proportional to $\frac{m_t}{m_b}$ and $\frac{m_c}{m_b}$ in the magnetic coefficients are neglected except the contribution coming from the virtual t-quark which gives $m_t = m_b$ enhancement. Also the term proportional to $\frac{m_t}{m_b}$ in the tree-level coefficient C_2^0 is not neglected because $\frac{m_t}{m_b} \approx 1$ and there is possible enhancement by the ratio of CKM angles ($\frac{V_{\text{td}}^{\text{RR}}}{V_{\text{td}}^{\text{LL}}} = \frac{V_{\text{td}}^{\text{LL}}}{V_{\text{td}}^{\text{RR}}}$) in the nonmanifest LR M .

The coefficients $C_i(\mu)$ at the scale $\mu = m_b$ can be obtained by evolving the coefficients $C_i(M_W)$ with the 28×28 anomalous dimension matrix applying the usual renormalization group procedure. Since the strong interaction preserves chirality, the 28×28 anomalous dimensional matrix decomposes into two identical 14×14 blocks. The SM 12×12 submatrix describing the mixing among $O_1 \dots O_{10}$, O_7 , and O_8^{G} can be found in Ref. [18], and the explicit form of the remaining 4×4 matrix describing the mixing among $O_{11,12}$, O_7 , and O_8^{G} , which partially overlaps with the SM 12×12 submatrix, can be found in Ref. [16]. The low energy Wilson coefficients at the scale $\mu = m_b$ in the LL approximation are then given by

$$C_i(m_b) = \sum_{j,k} (S^{-1})_{ij} (\lambda_j^{-23}) S_{jk} C_k(M_W); \quad (8)$$

where the λ_j 's in the exponent of $\lambda_j^{-23} = \lambda_j^{-23}(\mu) = \lambda_j^{-23}(m_b)$ are the eigenvalues of the anomalous dimension matrix over $g^2 = 16^{-2}$ and the matrix S contains the corresponding eigenvectors. The result for the photonic and gluonic magnetic coefficients are calculated in Ref. [16] and in Ref. [15], respectively, and the rest of them related to our analysis can be found in Ref. [17].² Therefore we do not repeat them here, and lead the reader to the original papers. For 5 flavors, we have the following numerical values of $C_i(m_b)$ in LL precision using $\overline{m_s} = 225$ MeV, $m_b = 4.4$ GeV, and $m_t = 170$ GeV:³

$$C_1^{\text{q}} = 0.308; \quad C_1^{\text{q0}} = C_1^{\text{q}} \frac{V_{\text{td}}^{\text{RR}}}{V_{\text{td}}^{\text{LL}}} = \frac{V_{\text{td}}^{\text{LL}}}{V_{\text{td}}^{\text{RR}}};$$

$$C_2^{\text{q}} = 1.144; \quad C_2^{\text{q0}} = C_2^{\text{q}} \frac{V_{\text{td}}^{\text{RR}}}{V_{\text{td}}^{\text{LL}}} = \frac{V_{\text{td}}^{\text{LL}}}{V_{\text{td}}^{\text{RR}}};$$

²Although QCD correction factors in $C_{1,2}^0$ are different from those in $C_{1,2}$ in general [19], we use an approximation $\lambda_s(M_W) \approx \lambda_s(M_b)$ for simplicity, which will not change our result.

³The numbers we obtained for $C_7^{(0)}$ and $C_8^{\text{G}(0)}$ are slightly different from those in Ref. [15] because they used $m_t = m_b = 60$.

$$\begin{aligned}
C_3 &= 0.014; \quad C_4 = 0.030; \quad C_5 = 0.009; \quad C_6 = 0.038; \\
C_7 &= 0.045; \quad C_8 = 0.048; \quad C_9 = 1.280; \quad C_{10} = 0.328; \\
C_7 &= 0.317 \quad 0.546A^{tb}; \quad C_7^0 = 0.546A^{ts}; \\
C_8^G &= 0.150 \quad 0.241A^{tb}; \quad C_8^{G0} = 0.241A^{ts};
\end{aligned} \tag{9}$$

Note that C_3^0 C_{10}^0 are negligible comparing to C_7^0 and C_8^{G0} whereas $C_{1,2}^0$ are not. We will show that $C_{1,2}^0$ are important to the absorptive parts in penguin-dominated B decays in the next section.

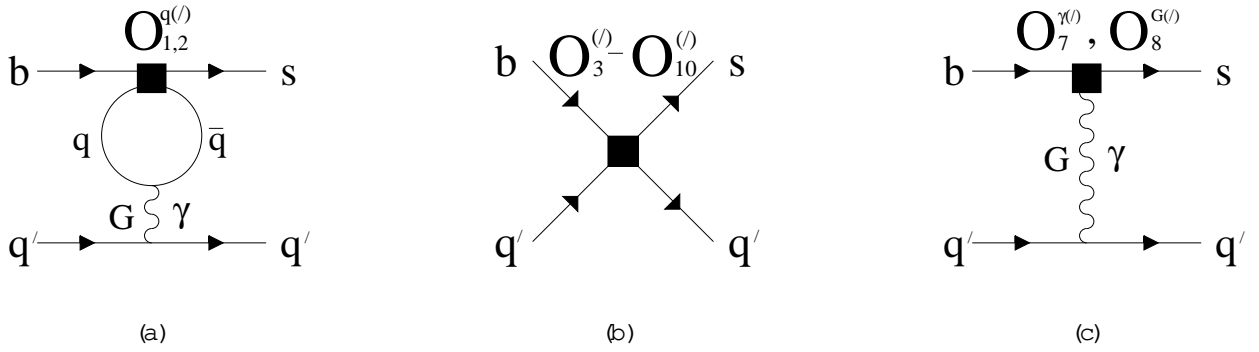


Figure 1: Diagrams for penguin-induced $b \rightarrow s q' \bar{q}$ decays.

3 CP violating asymmetries

3.1 Charged B meson decays

For charged B meson decays, the non-zero CP violating asymmetry defined as

$$A_{CP} = \frac{\Gamma(B^+ \rightarrow f^+) - \Gamma(B^- \rightarrow \bar{f})}{\Gamma(B^+ \rightarrow f^+) + \Gamma(B^- \rightarrow \bar{f})} \tag{10}$$

originates from the superposition of CP-odd (violating) phases introduced by CKM matrix elements and CP-even (conserving) phases arising from the absorptive part of the amplitudes. Since we have obtained the relevant effective Hamiltonian in Sec. 2, it is quite straightforward to calculate the partial decay rates and CP asymmetries in $b \rightarrow s s s$ decays. These decays are governed by three different types of penguin diagrams shown in Fig. 1. The absorptive part of the amplitudes arises at $O(\alpha_s)$ from the one-loop penguin diagrams with insertions

of the operators $O_{1,2}^{(0)}$ shown in Fig. 1 (a). The detailed calculation of the one-loop penguin matrix element of the operators $O_{1,2}$ in the SM is in Ref. [20] so that we can be very brief. The renormalized matrix elements of the operators $O_{1,2}^{(0)}$ in the LL approximation are given by

$$\begin{aligned}\langle O_1^{q(0)} \rangle^{\text{peng}} &= \frac{1}{3} I(m_q; k; m_b) \langle P^{(0)} \rangle; \\ \langle O_2^{q(0)} \rangle^{\text{peng}} &= \frac{s(m_b)}{8} I(m_q; k; m_b) \langle P_G^{(0)} \rangle + \frac{8}{9 s(m_b)} \langle P^{(0)} \rangle; \end{aligned} \quad (11)$$

where

$$\begin{aligned}P_G^{(0)} &= O_4^{(0)} + O_6^{(0)} - \frac{1}{N_c} (O_3^{(0)} + O_5^{(0)}); \\ P^{(0)} &= O_7^{(0)} + O_9^{(0)} \quad (N_c = 3); \end{aligned} \quad (12)$$

and

$$I(m; k;) = 4 \int_0^1 dx x (1-x) \ln \frac{h m^2 - k^2 x (1-x)}{2}; \quad (13)$$

and where k is the momentum transferred by the gluon to the $(s; s)$ pair. As one can see from Eq. 13, different CP-even phases arise from the imaginary parts of the functions $I(m_u; k;)$ and $I(m_c; k;)$. On the other hand, the penguin operators $O_3 - O_{10}$ contribute to only the dispersive parts of the amplitudes and give tree-level penguin transition amplitudes shown in Fig. 1 (b). Also, as shown in Fig. 1 (c), we should include the tree-level diagram associated with the magnetic operators $O_7^{(0)}$ and $O_8^{(0)}$ to the dispersive part of the amplitude. Using the factorization approximation [21], we use the following parametrization:

$$\begin{aligned}\langle O_7^{(0)} \rangle^{\text{peng}} &= \frac{m_b^2}{3 k^2} \langle P^{(0)} \rangle; \\ \langle O_8^{(0)} \rangle^{\text{peng}} &= \frac{s m_b^2}{4 k^2} \langle P_G^{(0)} \rangle; \end{aligned} \quad (14)$$

Here k^2 is expected to be typically in the range $m_b^2 = 4 k^2 = m_b^2 = 2$ [22]. We will use $k^2 = m_b^2 = 2$ for our numerical analysis.

Now we are ready to consider $B \rightarrow K$ decays explicitly. Since the axial-vector parts of the operators do not contribute to the transition amplitudes in these decays we can simply use $\langle O_i \rangle = \langle O_i^0 \rangle$ with the help of the vacuum insertion method [23]. Combining all operators, we obtain the following transition amplitude using the unitarity relation $\sum_{q=u,c,t} \langle O_i \rangle = 0$:

$$A(B \rightarrow K) = \frac{G_F}{2} \sum_{q=u,c}^{LL} \frac{s(m_b)}{9} C_2^q(m_b)$$

$$\begin{aligned}
& \frac{7}{6} \frac{(m_b)^n}{s(m_b)} (3C_1^q(m_b) + C_2^q(m_b)) I(m_q; k; m_b) \\
& - \frac{(m_b)^n}{9} 4C_8^G(m_b) - \frac{7}{s(m_b)} C_7(m_b) \\
& + \frac{4}{3} (C_3(m_b) + C_4(m_b)) + C_5(m_b) + \frac{1}{3} C_6(m_b) \\
& - \frac{1}{2} C_7(m_b) - \frac{1}{6} C_8(m_b) - \frac{2}{3} (C_9(m_b) + C_{10}(m_b)) \\
& \times X^{(B \rightarrow K; \gamma)} + (C_i - C_i^0);
\end{aligned} \tag{15}$$

where $X^{(B \rightarrow K; \gamma)} = \langle j_s s | \gamma \rangle \langle K | j_s b | B \rangle$. The amplitude $A^{(B^+ \rightarrow K^+)}$ is simply obtained from $A^{(B \rightarrow K)}$ by replacing $\frac{L^L}{q} \rightarrow \frac{L^L}{q}$ and $C_i^0 \rightarrow C_i^0$. In the SM, non-zero CP asymmetry arises from the superposition of the CP-odd phase in V_{ub}^L and the different CP-even phases arising from the function $I(m_q; k; m_b)$ due to the mass difference between c- and u-quark. The resulting CP asymmetry is known to be very small ($\sim 10^{-2}$) [20, 24] because the magnitude of the absorptive part is much smaller than that of the dispersive part. Using the numbers in Eq. 9, $m_c = 1.3 \text{ GeV}$, and $\text{Arg}[V_{ub}^L] = -59^\circ$, we can estimate the SM value of CP asymmetry:

$$A_{CP}^{SM}(B \rightarrow K) \sim 7.3 \times 10^{-3}. \tag{16}$$

If the model has manifest left-right symmetry, the W_R mass has a stringent bound $M_{W_R} \sim 1.6 \text{ TeV}$ [25], and its contribution to the decay amplitude is very small so that CP asymmetry in the manifest LRM should be very small as well. Since this value is small and our purpose is to estimate the possible large right-handed current contribution, we take a limit $I(m_c; k; \gamma) = I(m_u; k; \gamma)$ in order to get around the uncertainty of V_{ub}^L obtained under the SM framework and clearly see the right-handed current contribution. Then we can express $A^{(B \rightarrow K)}$ in terms of new parameters ρ , ϕ , and θ for two types of V^R in Eq. (4) in the LRM using the unitarity relation $\sum_{q=u,c,t} V_{q\gamma} = 0$ and the numbers in Eq. 9 again as follows:

$$\begin{aligned}
A^{(B \rightarrow K)}_I & \sim \frac{G_F}{\sqrt{2}} \left[2.87 e^{i\phi_1} + 23.1 e^{i\phi_2} \rho g_R s_R e^{i(\phi_4 - \phi_3)} \right. \\
& \left. + 10.1 \rho (g_R e^{i\phi_4} - 25.8 e^{i\phi_3}) \right] \times 10^3 X^{(B \rightarrow K; \gamma)}; \\
A^{(B \rightarrow K)}_{II} & \sim \frac{G_F}{\sqrt{2}} \left[2.87 e^{i\phi_1} + 10.1 \rho g_R e^{i\phi_4} \right] \times 10^3 X^{(B \rightarrow K; \gamma)};
\end{aligned} \tag{17}$$

where $(\phi_1, \phi_2) = (14.9^\circ, 53.1^\circ)$ are CP-even phases. As stated earlier, one can clearly see here that the ρ term coming from the coefficients $C_{1,2}^0$ is not negligible in case of V_I^R .

Likewise, the transition amplitude in $B \rightarrow K$ decays can be easily obtained by using $\langle O_i \rangle = \langle O_i^0 \rangle$ because K is a vector particle:

$$\begin{aligned}
 A(B \rightarrow K)_I &= \frac{G_F}{\sqrt{2}} \left[2.87e^{i\gamma_1} + 23.1e^{i\gamma_2} g_{CR} s_R e^{i(\gamma_4 - \gamma_3)} \right. \\
 &\quad \left. + 10.1 g_{CR} (e^{i\gamma_4} - 25.8e^{i\gamma_3}) \right] 10^3 X^{(B \rightarrow K)}; \\
 A(B \rightarrow K)_{II} &= \frac{G_F}{\sqrt{2}} \left[2.87e^{i\gamma_1} - 10.1 g_{CR} e^{i\gamma_4} \right] 10^3 X^{(B \rightarrow K)};
 \end{aligned} \tag{18}$$

where $X^{(B \rightarrow K)} = \langle \bar{\psi} \psi \rangle / \langle K | \bar{\psi} \psi | B \rangle$. Although the CP asymmetry in $B \rightarrow K$ decays should be the same as that in $B \rightarrow K$ decays in the SM, they can be different in LRM so that the measured difference of CP asymmetries between them may give the size of the NP effects.

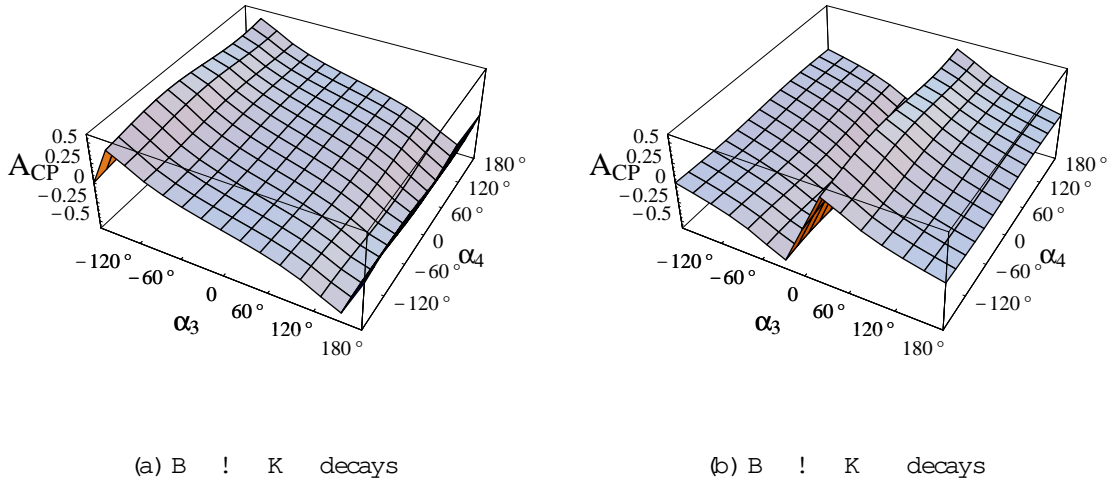


Figure 2: Behavior of A_{CP} as $\alpha_{3,4}$ are varied in the case of V_I^R .

The current data on the CP asymmetries in $B \rightarrow K$ and $B \rightarrow K$ decays are [26]:

$$\begin{aligned}
 A_{CP}^{\text{expt}}(B \rightarrow K) &= 0.05 \pm 0.20 \pm 0.03; \\
 A_{CP}^{\text{expt}}(B \rightarrow K) &= 0.43^{+0.36}_{-0.30} \pm 0.06;
 \end{aligned} \tag{19}$$

The SM value in Eq. (16) lies in the range of $A_{CP}^{\text{expt}}(B \rightarrow K)$, but a little out of the range of $A_{CP}^{\text{expt}}(B \rightarrow K)$. In order to explicitly compare these values with the theoretical estimates in the LRM, we first plot $A_{CP}(B \rightarrow K)$ and $A_{CP}(B \rightarrow K)$ in the

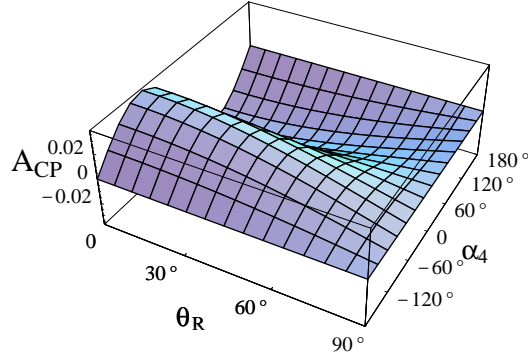


Figure 3: Behavior of $A_{CP}(B \rightarrow K^0)$ as θ_R and α_4 are varied in the case of V_{II}^R .

case of V_I^R in Fig. 2 for the typical values $\theta_g = 0.01$, $\alpha_g = 0.008$, and $\theta_R = 70^\circ$ as $\alpha_{3,4}$ are varied. In the figure, CP asymmetry is drastically changing by varying α_3 , and this behavior holds for other values of θ_g , α_g , and θ_R . For the given inputs, $A_{CP}(B \rightarrow K^0)$ and $A_{CP}(B \rightarrow \bar{K}^0)$ can be different by about 0.5. In the case of V_{II}^R , one can see from Eqs. (18), (19) that $A_{CP}(B \rightarrow K^0) = A_{CP}(B \rightarrow \bar{K}^0)$ because it has no dependence of θ_g and α_3 unlike the previous case. In Fig. 3, we fix $\theta_g = 0.01$, and evaluate CP asymmetry by varying θ_R and α_4 . It shows that CP asymmetry is very small with a small parameter θ_g . Therefore, if we observe large CP asymmetry or any difference between $A_{CP}(B \rightarrow K^0)$ and $A_{CP}(B \rightarrow \bar{K}^0)$, the second type of mass mixing matrix V_{II}^R is disfavored.

3.2 Neutral B meson decays

In the case of the neutral B meson decays into CP self-conjugate final states f , mixing induced CP asymmetry can be expressed by the parametrization invariant quantity defined by [1]

$$\mathcal{A}_f = \frac{q}{p_B} \frac{A(B^0 \rightarrow f)}{A(\bar{B}^0 \rightarrow f)}; \quad \frac{q}{p_B} = e^{i\phi} \frac{M_{12}}{M_{12}^*}; \quad (20)$$

where $\mathcal{A}_f = 1(-1)$ for a CP-even(odd) final state f and M_{12} is the dispersive part of the $B\bar{B}$ mixing matrix element. The CP angle mentioned earlier is simply the imaginary part of ϕ in $B \rightarrow J/\psi K_S$ decays in the SM :

$$\sin 2\phi = \text{Im}(B \rightarrow J/\psi K_S) / \text{Im}(B \rightarrow K_S): \quad (21)$$

In the general LRM, M_{12} can be written as

$$M_{12} = M_{12}^{SM} + M_{12}^{LR} = M_{12}^{SM} + r_{LR} M_{12}^{SM}; \quad (22)$$

where

$$r_{LR} = \frac{M_{12}^{LR}}{M_{12}^{SM}} = \frac{\langle B^0 | H_{eff}^{LR} | \bar{B}^0 \rangle}{\langle B^0 | H_{eff}^{SM} | \bar{B}^0 \rangle}; \quad (23)$$

with the effective Hamiltonian $H_{eff}^{BB} = H_{eff}^{SM} + H_{eff}^{LR}$ in the $B\bar{B}$ system. Considering the two types of the quark mixing matrices in Eq. (4), the effective Hamiltonians in the $B\bar{B}$ system are given by

$$H_{eff}^{SM} = \frac{G_F^2 M_W^2}{4} (V_{cb}^L)^2 S(x_t^2) (d_L \bar{b}_L)^2; \quad (24)$$

$$H_{eff}^{LR} = \frac{G_F^2 M_W^2}{2} \{ f_c^{LR} V_{cb}^{RL} x_t^2 A_1(x_t^2) + V_{cb}^{LR} V_{cb}^{RL} x_t^2 A_2(x_t^2) g(d_L \bar{b}_R)(d_R \bar{b}_L) + V_{cb}^{LR} V_{cb}^{RL} x_t^2 A_3(x_t^2) (d_L \bar{b}_L)(d_R \bar{b}_R) + x_t^2 A_4(x_t^2) (d_L \bar{b}_R)(d_R \bar{b}_L) g \}; \quad (25)$$

where $S(x)$ is the usual Inami-Lin function and A_i can be found in Ref. [5]. If we consider QCD effect in $B\bar{B}$ mixing, the correction factors should be included in the functions S and A_i . However, there are many uncertainties such as hadronic matrix elements and new parameters in the LRM to prevent us from the precision analysis at this stage, and the QCD corrections to $B\bar{B}$ mixing are not big enough to change our numerical estimate. Therefore we will ignore the QCD corrections to $B\bar{B}$ mixing for simplicity. In the case of V_I^R , there is no significant contribution of H_{eff}^{LR} to $B\bar{B}$ mixing, so that $M_{12} = M_{12}^{SM}$ because $V_{cb}^{RL} = 0$. In the case of V_{II}^R , using $m_c = 1.3 \text{ GeV}$, $m_b = 4.4 \text{ GeV}$, $m_t = 170 \text{ GeV}$, and $|V_{cd}^L| = 0.224$, and adopting the parameterization of the hadronic matrix elements of the operators given in Ref. [5], one can express r_{LR} in terms of the mixing angle and phases in Eq. (4) as

$$r_{LR} = \frac{1}{1.1731} \frac{1 - g \frac{(4.92 - 19.7g) \ln(1-g)}{1 - 5.47g}}{796 \frac{1 - 5.02g \frac{(0.498 - 1.99g) \ln(1-g)}{1 - 9.94g + 28.9g^2}}{g s_R^2 e^{i\phi_1} + g s_R c_R e^{i\phi_2} + 8.93 g s_R e^{i\phi_3}}}; \quad (26)$$

where $1 = 0.008 = |V_{td}^L|$, $\phi_1 = \phi_2 + \phi_3$, $\phi_2 = \phi_3 + \phi_4$, $\phi_3 = \phi_4$. Since $B \rightarrow J/\psi K_S$ decay is governed by the tree-level amplitude, the transition amplitude is given by

$$A(B \rightarrow J/\psi K_S)_I = \frac{G_F}{\sqrt{2}} V_{cb}^{LL} [1 + 25 (c_R s_R g e^{i(\phi_2 - \phi_1)} - 2 s_R g e^{i\phi_2}) X^{(BK_S, J=\psi)}];$$

$$A(B \rightarrow J=K_S)_{II} = \frac{G_F}{\sqrt{2}} V_c^{LL} \frac{n}{1} 50 s_g e^{i\alpha_2} X^{(B K_S; J=)}; \quad (27)$$

where $X^{(B K_S; J=)} = \langle J= | c\bar{c} | \rangle \langle K_S | \bar{s} b | \rangle$, and we ignored the $K\bar{K}$ mixing. The transition amplitude in $B \rightarrow K_S$ decays can be simply obtained from Eq. (18) by replacing the hadronic matrix element $X^{(B K;)} \rightarrow X^{(B K_S;)}$.

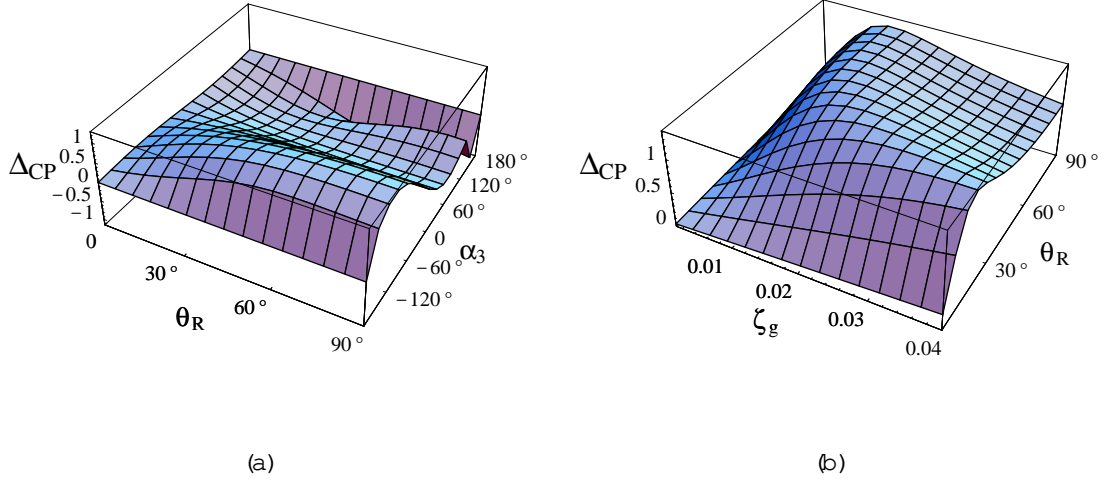


Figure 4: Behavior of the CP asymmetry difference Δ_{CP} between $B \rightarrow J=K_S$ and $B \rightarrow K_S$ decays in the case of V_I^R .

For illustration of the possible effect of the new interaction on the mixing induced CP asymmetry, we assume that $\alpha = 20^\circ$ and $l = 1$, and show that the region of parameters α_3 where $\text{Im}(B \rightarrow J=K_S) \geq 0.73$ and $\text{Im}(B \rightarrow K_S) \geq 0.39$ since $|j| \leq 1$. To do so, we need to find an appropriate set of parameters s_g , α_3 , and θ_R yielding a large difference $\Delta_{CP} = \text{Im}(B \rightarrow J=K_S) - \text{Im}(B \rightarrow K_S)$. First, we evaluate Δ_{CP} in the case of V_I^R for $s_g = s_g = 0.01$, $\alpha_2 = 0$ by varying θ_R and α_3 in Fig. 4(a). In the figure, Δ_{CP} becomes maximal near $\alpha_3 \approx 120^\circ$ and increases as θ_R increases, and this behavior holds for other values of fixed parameters. Since we assumed that Δ_{CP} is larger than 1, we fix $\alpha_3 = 120^\circ$, and evaluate Δ_{CP} in Fig. 4(b) for $\alpha_2 = 0$ and $s_g = s_g$ by varying θ_R and s_g . One can see from the figure that Δ_{CP} approaches 1 for $s_g \approx 0.01$ and $\theta_R \approx 10^\circ$, and its variation is small. After repeating this analysis, we get a probable set of parameter values $s_g = 0.01$, $s_g = 0.008$, $\theta_R = 70^\circ$, and $\alpha_3 = 120^\circ$. Using these values, we plot the contours corresponding to $\text{Im}(B \rightarrow J=K_S) = 0.73$ and $\text{Im}(B \rightarrow K_S) = 0.39$ in the parameter space of α_2 in Fig. 5. Therefore, as a result from the obtained figures, the manifest or

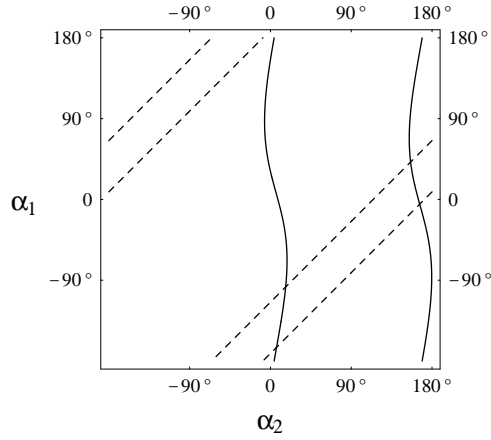


Figure 5: Contour plot corresponding to $\text{Im}(B \rightarrow J=K_S) = 0.73$ (solid line) and $\text{Im}(B \rightarrow K_S) = 0.39$ (dashed line) for $\sin 2\theta = 0.64$ in the case of V_I^R .

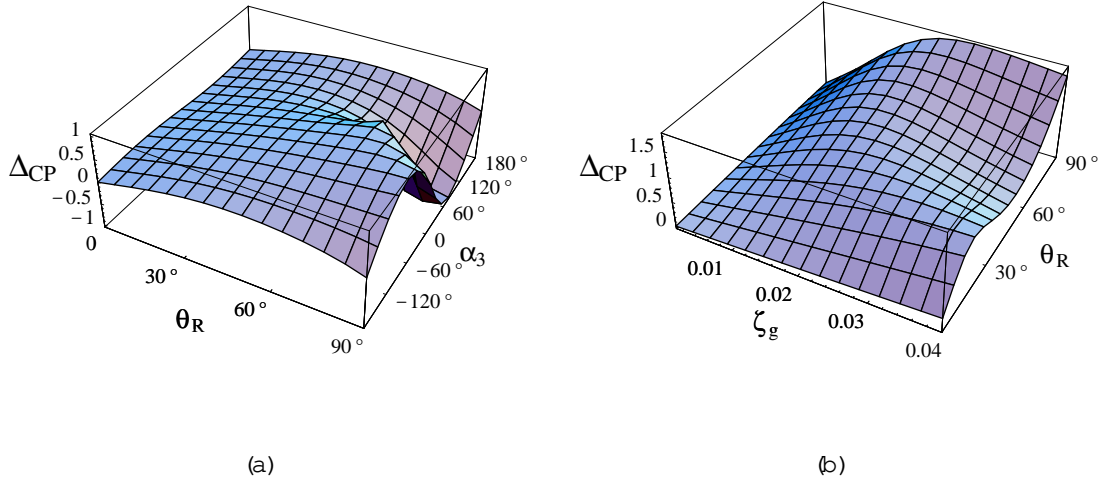


Figure 6: Behavior of the CP asymmetry difference Δ_{CP} between $B \rightarrow J=K_S$ and $B \rightarrow K_S$ decays in the case of V_{II}^R .

pseudomanifest LRM is disfavored under the given assumption. In a similar way to the case of V_I^R , the results of the analysis of the mixing induced CP asymmetries in the case of V_{II}^R are represented in Fig. 6 and Fig. 7.

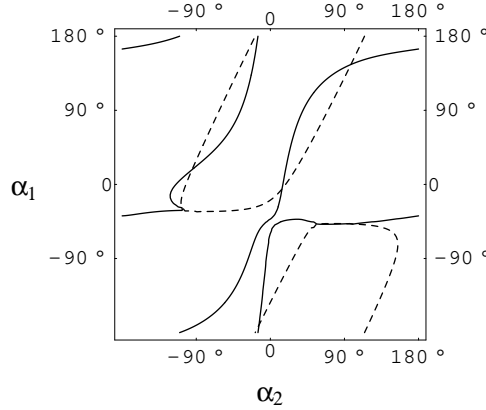


Figure 7: Contour plot corresponding to $\text{Im}(B \rightarrow J=K_s) = 0.73$ (solid line) and $\text{Im}(B \rightarrow K_s) = 0.39$ (dashed line) for $\sin 2\beta = 0.64$ in the case of V_{II}^R .

4 Conclusions

In this paper, we studied CP asymmetries in penguin-induced $b \rightarrow sss$ decays in the general LRM. Without imposing manifest or pseudomaniest left-right symmetry, one has two types of mass mixing matrix V^R with which the right-handed current contributions to BB mixing and CP asymmetry can be sizable even in the decays such as $B \rightarrow K^{(*)}$ decays where the SM contribution to CP asymmetry is very small. Using the effective Hamiltonian approach, we evaluate the sizes of the NP contributions to CP asymmetries in $B \rightarrow K^{(*)}$ decays, and show that V_I^R is more probable than V_{II}^R if CP asymmetries in those decays are large or different from each other. Similar argument can be made in mixing induced B decays such as $B \rightarrow J=K_s$ and $B \rightarrow K_s$ decays. Although SM predicts that the CP asymmetry in $B \rightarrow J=K_s$ decays should be very close to that in $B \rightarrow K_s$ decays, the present experiments show a large discrepancy between them. Based on these preliminary experimental results, we find that the manifest or pseudomaniest LRM is disfavored, and the bounds of the new parameters are restricted as shown in Figs. 4–7. Furthermore, this result may affect the sizes of CP asymmetries in other decays. For instance, one can see from Fig. 2 and Fig. 3 that the contributions of the obtained parameter sets from Fig. 5 and Fig. 7 under the given assumption reduces the size of CP asymmetries in $B \rightarrow K$ decays. In this way, CP asymmetries in other mixing induced decays such as $B \rightarrow K$ can be estimated systematically, and all of these analysis of possible NP contributions can be tested once the

experimental results are confirmed.

5 Acknowledgements

The author would like to thank M. B. Voloshin for careful reading of the manuscript and his valuable comments. This work is supported in part by the DOE grant DE-FG 02-94ER 40823.

References

- [1] For a recent review, see I.I. Bigi and A.I. Sanda, *CP Violation* (Cambridge University Press, Cambridge, England, 2000).
- [2] Y.Nir, *Nucl. Phys. Proc. Suppl.* 117, 111 (2003).
- [3] BABAR Collaboration, B.Aubert et al, *hep-ex/0207070*; Belle Collaboration, K.Abe et al, *hep-ex/0207098*.
- [4] Y.Grossman and M.P.Worah, *Phys. Lett. B* 395, 241 (1997); Y.Grossman, G.Isidori and M.P.Worah, *Phys. Rev. D* 58, 057504 (1998).
- [5] S.-h.Nam, *Phys. Rev. D* 66, 055008 (2002).
- [6] J.C.Pati and A.Salam, *Phys. Rev. D* 10, 275 (1974); R.N.Mohapatra and J.C.Pati, *ibid.* 11, 566 (1975); 11, 2558 (1975).
- [7] B.Balke et al, *Phys. Rev. D* 37, 587 (1988).
- [8] CDF Collaboration, F.Abe et al, *Phys. Rev. Lett.* 74, 2900 (1995); D Collaboration, S.Abachi et al, *Phys. Rev. Lett.* 76, 3271 (1996).
- [9] For a review, see P.Langacker and S.J.Sankar, *Phys. Rev. D* 40, 1569 (1989).
- [10] For a review, see R.N.Mohapatra, *Unification and Supersymmetry* (Springer, New York, 1992).
- [11] F.I.Ohness and M.E.Ebel, *Phys. Rev. D* 30, 1034 (1984); D.London and D.Wyller, *Phys. Lett. B* 232, 503 (1989); also see Ref. [9].
- [12] M.B.Voloshin, *Mod. Phys. Lett. A* 12, 1823 (1997).
- [13] J.Chay, K.Y.Lee, and S.-h.Nam, *Phys. Rev. D* 61, 035002 (1999); also see Ref. [10].
- [14] D.Chang, J.Basecq, L.-F.Li, and P.B.Pal, *Phys. Rev. D* 30, 1601 (1984).
- [15] G.Barenboim, J.Bernabeu, and M.Raidal, *Phys. Rev. Lett.* 80, 4625 (1998); G.Barenboim, J.Bernabeu, J.Matias, and M.Raidal, *Phys. Rev. D* 60, 016003 (1999); M.Raidal, *Phys. Rev. Lett.* 89, 231803 (2002).

- [16] P. Cho and M. Misiak, Phys. Rev. D 49, 5894 (1994).
- [17] G. Buchalla, A. J. Buras, and M. Lautenbacher, Rev. Mod. Phys. 68, 1125 (1996); A. J. Buras, hep-ph/9806471.
- [18] M. Ciuchini et al., Phys. Lett. B 316, 127 (1993); Nucl. Phys. B 415, 403 (1994); also see Ref. [17].
- [19] G. Ecker and W. Grimus, Nucl. Phys. B 258, 328 (1985).
- [20] R. Fleischer, Z. Phys. C 58, 483 (1993); *ibid.* 62, 81 (1994).
- [21] M. Bauer, B. Stech, and M. Wirbel, Z. Phys. C 29, 637 (1985); *ibid.* 34, 103 (1987); A. Ali and C. Greub, Phys. Rev. D 57, 2996 (1998).
- [22] N. G. Deshpande and J. Trampetic, Phys. Rev. D 41, 2926 (1990); H. Simma and D. Wyler, Phys. Lett. B 272, 395 (1991).
- [23] M. K. Gaillard and B. W. Lee, Phys. Rev. D 10, 897 (1974);
- [24] A. Ali, G. Kramer, and C.-D. Lu, Phys. Rev. D 59, 014005 (1998).
- [25] G. Beall, M. Bander, and A. Soni, Phys. Rev. Lett. 48, 848 (1982).
- [26] BABAR Collaboration, B. Aubert et al., Phys. Rev. D 65, 051101 (2002).